

SCIENTIFIC REPORTS



OPEN

Opportunistic Entanglement Distribution for the Quantum Internet

Laszlo Gyongyosi^{1,2,3} & Sandor Imre²

Quantum entanglement is a building block of the entangled quantum networks of the quantum Internet. A fundamental problem of the quantum Internet is entanglement distribution. Since quantum entanglement will be fundamental to any future quantum networking scenarios, the distribution mechanism of quantum entanglement is a critical and emerging issue in quantum networks. Here we define the method of opportunistic entanglement distribution for the quantum Internet. The opportunistic model defines distribution sets that are aimed to select those quantum nodes for which the cost function picks up a local minimum. The cost function utilizes the error patterns of the local quantum memories and the predictability of the evolution of the entanglement fidelities. Our method provides efficient entanglement distributing with respect to the actual statuses of the local quantum memories of the node pairs. The model provides an easily-applicable, moderate-complexity solution for high-fidelity entanglement distribution in experimental quantum Internet scenarios.

Quantum entanglement has a central role in the quantum Internet^{1–10}, quantum networking^{11–26}, and long-distance quantum key distribution^{1,19,27,28}. Entanglement distribution is a crucial phase for the construction of the entangled core network structure of the quantum Internet. In a quantum Internet scenario, quantum entanglement is a preliminary condition of quantum networking protocols^{27,29–44}. Distant quantum nodes that share no quantum entanglement must communicate with their direct neighbors to distribute entanglement. To aim of entanglement distribution is to generate entanglement between a distant source node and a target node through a chain of intermediate quantum repeater nodes^{45–57}. The intermediate quantum repeater nodes receive the entangled states, store them in their local quantum memories^{28,58,59}, and apply a unitary operation (called entanglement swapping^{1–3,19}) to extend the range of quantum entanglement. Storing quantum entanglement in the quantum nodes' local quantum memories adds noise to the distribution process, since quantum memories are non-perfect devices^{34,60} and the error probabilities evolve in time^{1,49–54}. As the error pattern of the evolution the quantum memories is predictable, the nodes can be characterized by a given storage success probability after a given time from the start of the storage.

The fidelity of entanglement^{61–63} is another critical parameter for entanglement distribution. In a quantum network with a chain of repeater nodes between a source and target nodes, for all pairs of entangled nodes (e.g., for nodes that share a common entanglement) a given lower bound in the fidelity of entanglement must be satisfied, otherwise the entanglement distribution fails^{1,64}. The stored entangled states have a given amount of fidelity that is determined by the transmission procedure, such as the noise of the quantum channel, etc. The evolution of a given entangled system's fidelity parameter is time-varying in quantum memory, since it evolves through time, from the beginning of storage to the actual current time. Therefore, it is necessary to consider the predictability of the evolution of both the error patterns of the nodes' local quantum memories, and the evolution of the stored quantum states' fidelity of entanglement. In our model, using these parameters, we define an appropriate cost function for the realization of entanglement distribution.

Here we define the method of opportunistic entanglement distribution for the quantum Internet. The proposed scheme utilizes a cost function that accounts for the error patterns of local quantum memories and also the evolution of entanglement fidelities. The opportunistic model defines distribution sets in the entangled quantum network of the quantum Internet. A distribution set contains those quantum nodes for which our cost function

¹School of Electronics and Computer Science, University of Southampton, Southampton, SO17 1BJ, UK. ²Department of Networked Systems and Services, Budapest University of Technology and Economics, Budapest, H-1117, Hungary. ³MTA-BME Information Systems Research Group, Hungarian Academy of Sciences, Budapest, H-1051, Hungary. Correspondence and requests for materials should be addressed to L.G. (email: l.gyongyosi@soton.ac.uk)

picks up a local minimum in comparison to the cost of the other nodes in the given distributing set. The distribution set selects a lowest-cost node from a given set of nodes to provide a maximal usability of stored entanglement. The cost function ensures that the nodes selected for entanglement distribution allow the lowest deviation in the entanglement fidelity from the start of storage, and that the behavior of the quantum memory error follows a predicted error model with respect to a given node pair. We also derive the computational complexity of the proposed method. The solution provides an easily-applicable, low-complexity solution for high-fidelity entanglement distribution in the quantum Internet.

The novel contributions of our manuscript are as follows:

1. We define the method of opportunistic entanglement distribution for the quantum Internet.
2. The proposed opportunistic model defines distribution sets that are aimed to select those quantum nodes for which the cost function picks up a local minimum. The cost function utilizes the error patterns of the local quantum memories and the predictability of the evolution of the entanglement fidelities.
3. Our method provides efficient entanglement distributing with respect to the actual statuses of the local quantum memories of the node pairs.
4. We derive the computational complexity of the model.

This paper is organized as follows. In Section 2 the preliminaries are summarized. Section 3 defines the method, while Section 4 proposes the results. Finally, Section 5 concludes the results.

Preliminaries

System Model. The quantum Internet setting is modeled as follows⁸. Let V refer to the nodes of an entangled quantum network N , with a transmitter quantum node $A \in V$, a receiver quantum node $B \in V$, and quantum repeater nodes $R_i \in V, i = 1, \dots, q$. Let $E = \{E_j\}, j = 1, \dots, m$, refer to a set of edges between the nodes of V , where each E_j identifies an L_r -level entangled connection, $l = 1, \dots, r$, between quantum nodes x_j and y_j of edge E_j , respectively. The entanglement levels of the entangled connections in the entangled quantum network structure are defined as follows.

Entanglement Levels. In a quantum Internet setting, an $N = (V, E)$ entangled quantum network consists of single-hop and multi-hop entangled connections, such that the single-hop entangled nodes (The l -level entangled nodes x, y refer to quantum nodes x and y connected by an entangled connection L_l) are directly connected through an L_1 -level entanglement, while the multi-hop entangled nodes communicate through L_r -level entanglement. Focusing on the doubling architecture¹⁻³ in the entanglement distribution procedure, the number of spanned nodes is doubled in each level of entanglement swapping (entanglement swapping is applied in an intermediate node to create a longer distance entanglement¹). Therefore, the $d(x, y)_{L_l}$ hop distance in N for the L_r -level entangled connection between $x, y \in V$ is denoted by⁸

$$d(x, y)_{L_l} = 2^{l-1}, \quad (1)$$

with $d(x, y)_{L_l} - 1$ intermediate quantum nodes between x and y . Therefore, $l = 1$ refers to a direct entangled connection between two quantum nodes x and y without intermediate quantum repeaters, while $l > 1$ identifies a multilevel entanglement.

An entangled quantum network N is illustrated in Fig. 1. The quantum network integrates single-hop entangled nodes (depicted by gray nodes) and multi-hop entangled nodes (depicted by blue and orange nodes) connected by edges. The single-hop entangled nodes are directly connected through an L_1 -level entangled connection, while the multi-hop entangled nodes are connected by L_2 and L_3 -level entangled connection.

The fidelity of entanglement of an L_r -level entangled connection $E(x, y)$ between $x, y \in V$ depends on the physical attributes of the quantum network.

Terms and Definitions. *Entanglement Fidelity.* Let

$$|\beta_{00}\rangle = \frac{1}{\sqrt{2}}(|00\rangle + |11\rangle) \quad (2)$$

be the target Bell state subject to be created at the end of the entanglement distribution procedure between a particular source node A and receiver node B . The entanglement fidelity F at an actually created noisy quantum system σ between A and B is

$$F(\sigma) = \langle \beta_{00} | \sigma | \beta_{00} \rangle, \quad (3)$$

where F is a value between 0 and 1, $F = 1$ for a perfect Bell state and $F < 1$ for an imperfect state. Without loss of generality, in an experimental quantum Internet setting, an aim is to reach $F \geq 0.98$ over long distances^{1,3}.

Some properties of F are as follows^{4,19}. The fidelity for two pure quantum states $|\varphi\rangle, |\psi\rangle$ is defined as

$$F(|\varphi\rangle, |\psi\rangle) = |\langle \varphi | \psi \rangle|^2. \quad (4)$$

The fidelity of quantum states can describe the relation of a pure state $|\psi\rangle$ and mixed quantum system $\sigma = \sum_{i=0}^{n-1} p_i \rho_i = \sum_{i=0}^{n-1} p_i |\psi_i\rangle \langle \psi_i|$, as

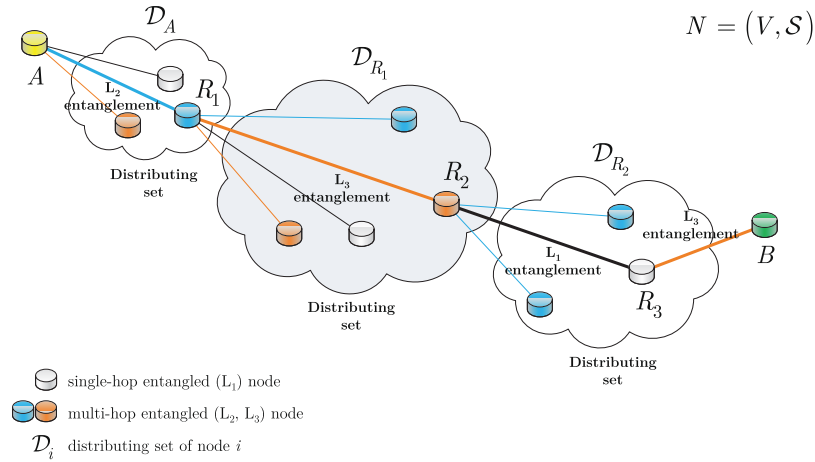


Figure 1. Opportunistic entanglement distribution in a quantum Internet setting, $N = (V, S)$. The entangled contacts of transmitter node A define the distributing set \mathcal{D}_A . From set \mathcal{D}_A , a quantum repeater node R_1 is selected. Node R_1 shares L_2 -level entanglement with A . The entangled contacts of the repeater node R_1 define the distributing set \mathcal{D}_{R_1} . The iteration is repeated until target node B is reached via a quantum repeater node. In this network setting, B is reached via node R_3 from set \mathcal{D}_{R_2} , where R_3 shares L_3 -level entanglement with B . Applying the opportunistic entanglement distribution for the nodes of the network, a path between A and B is selected (depicted in bold).

$$F(|\psi\rangle, \sigma) = \langle \psi | \sigma | \psi \rangle = \sum_{i=0}^{n-1} p_i |\langle \psi | \psi_i \rangle|^2. \tag{5}$$

Fidelity can also be defined for mixed states σ and ρ , as

$$F(\rho, \sigma) = (\text{Tr}(\sqrt{\sqrt{\sigma} \rho \sqrt{\sigma}}))^2 = \sum_i p_i \left(\text{Tr}(\sqrt{\sqrt{\sigma_i} \rho_i \sqrt{\sigma_i}}) \right)^2. \tag{6}$$

Method

Before giving the details of the algorithm, we briefly summarize the method of opportunistic entanglement distribution in a quantum Internet setting in Method 1.

Method 1. Opportunistic entanglement distribution in the quantum Internet.

- Step 1.** Select a cheapest quantum node i . Generate entanglement between i and the direct contacts of i . The entangled contacts of i define the distributing set \mathcal{D}_i of i .
 - Step 2.** From \mathcal{D}_i , select a cheapest quantum node j . Generate entanglement between j and the direct contacts of j to define \mathcal{D}_j . Select the cheapest node from \mathcal{D}_j .
 - Step 3.** Repeat steps 1-2 until the source and target nodes share entanglement.
-

Discussion. In Step 1, distributing entanglement between i and the direct contacts of i defines the distributing set \mathcal{D}_i , which can contain different levels of entangled contacts. In our opportunistic approach, the heterogenous entangled contacts leads to diverse hop-distances, specifically for an L_l -level entanglement $l = 1, \dots, r$, the $d(i, y)_{L_l}$, the hop-distance between a source node i and target node $D_i \in y$ from the distributing set \mathcal{D}_i is determined via (4) as $d(i, y)_{L_l} = 2^{l-11-3,8}$.

In Step 2, the next node j from a set \mathcal{D}_i is selected by the same cost metric used for the selection of node i in Step 1. The cost metric^{65,66} used in the opportunistic node selection procedure in Steps 1–2 ensures the selection of those nodes that can preserve the entangled quantum states with the highest fidelity in their local quantum memories. From a given distributing set \mathcal{D} , only one node is selected in each iteration step. The cost function will be clarified later in the algorithm.

Finally, Step 3 provides an iteration to reach from the source node to the target node.

Figure 1 illustrates the method of opportunistic entanglement distribution in a quantum repeater network N . A given distributing set \mathcal{D}_i of a node i can contain several different levels L_l of entangled contacts. From a distributing set \mathcal{D}_i , only one repeater node is selected in each level of iteration. Those quantum nodes that share L_1 -level entanglement are referred to as single-hop entangled nodes, while the other entangled nodes are referred to as multi-hop entangled nodes.

Ethics statement. This work did not involve any active collection of human data.

Results

Parameterization. Let \mathcal{D}_i be a distributing set of a node i , and let $p_{i,j}^{F^*}$ be the probability of the shared entanglement stored in the quantum memories of nodes (i, j) , where $j \in \mathcal{D}_i$ identifies a repeater node R_j from the distributing set \mathcal{D}_i , with a fidelity $F^* \geq F_{crit}$, where F_{crit} is a critical lower bound on the fidelity of entanglement.

Then, let $p_{i,\mathcal{D}_i}^{F^*}$ be the probability that $F^* \geq F_{crit}$ is satisfied between node i and at least one repeater node from \mathcal{D}_i . Using $p_{i,\mathcal{D}_i}^{F^*}$ and $p_{i,j}^{F^*}$, a cost function $f(p_{i,\mathcal{D}_i}^{F^*})$ can be defined^{65,66} as

$$f(p_{i,\mathcal{D}_i}^{F^*}) = \frac{1}{p_{i,\mathcal{D}_i}^{F^*}} = \frac{1}{1 - \prod_{j \in \mathcal{D}_i} (1 - p_{i,j}^{F^*})}. \tag{7}$$

Similarly, with $p_{\mathcal{D}_i,B}^{F^*}$ as the probability that there exists entanglement between a node $j \in \mathcal{D}_i$ of \mathcal{D}_i and the target node B with fidelity criterion $F^* \geq F_{crit}$, a cost function between a repeater node $j \in \mathcal{D}_i$ and a target node B can be defined as

$$f(p_{\mathcal{D}_i,B}^{F^*}) = \sum_{j \in \mathcal{D}_i} \phi_{i,j} f(p_{j,B}^{F^*}), \tag{8}$$

where $p_{j,B}^{F^*}$ is the probability of $F^* \geq F_{crit}$ fidelity entangled contact between a given $j \in \mathcal{D}_i$ and B , while $\phi_{i,j}$ is the probability that a given repeater node j is selected from \mathcal{D}_i for i , defined⁶⁶ as

$$\phi_{i,j} = \frac{p_{i,j}^{F^*} \prod_{k=1}^{j-1} (1 - p_{i,k}^{F^*})}{1 - \prod_{j \in \mathcal{D}_i} (1 - p_{i,j}^{F^*})}, \tag{9}$$

where

$$\sum_i \phi_{i,j} = 1. \tag{10}$$

From equations (7) and (8), the cost function between a quantum node i and a target node B at a distributing set \mathcal{D}_i , such that $F^* \geq F_{crit}$ holds for the fidelity of all entangled contacts from i to B , is therefore

$$f(p_{i,B}^{F^*}) = f(p_{i,\mathcal{D}_i}^{F^*}) + f(p_{\mathcal{D}_i,B}^{F^*}). \tag{11}$$

The $p_{i,j}^{F^*}$ probabilities depend on the actual state of the quantum memory (particularly, on the ε_i error probability of the quantum memory of node i) and on the F fidelity of the stored entanglement. Parameters ε and F are time-varying in our model, which is denoted by $\varepsilon(t)$ and $F(t)$, where t refers to the storage time in quantum memory. Time t_0 refers to the start of the storage of a quantum system in quantum memory.

Let $\varepsilon_{i,j}(t_0 + \Delta t)$ identify the error probability of quantum memories in nodes (i, j) such that $\varepsilon_{i,j} \in [0, \varepsilon_{crit}]$ holds, which allows storing an $F^* \geq F_{crit}$ fidelity entanglement in the nodes after Δt time from start time t_0 . Therefore, at a ε_{crit} critical upper bound on the quantum memories,

$$\varepsilon_{i,j}(t_0 + \Delta t) = |\zeta_i(t_0 + \Delta t) - \zeta_j(t_0 + \Delta t)| \leq \varepsilon_{crit} \tag{12}$$

holds, where $\zeta_i(t_0 + \Delta t)$ characterizes the change of the error probability of the quantum memory of node i at $t_0 + \Delta t$, as in

$$\zeta_i(t_0 + \Delta t) = \zeta_i(t_0) + \varphi_i(t_0, \Delta t), \tag{13}$$

where $\zeta_i(t_0)$ is the ε_i error probability of the quantum memory of node i at t_0 , while $\varphi_i(t_0, \Delta t)$ is the change of ε_i from t_0 to $t_0 + \Delta t$.

Let $\eta_i(t) = (\varepsilon_i(t), 1 - F_i(t))$ identify the $\varepsilon_i(t)$ quantum memory error probability and the $F_i(t)$ stored entanglement fidelity in node i at time t . Then, the $d_{i,j}$ distance between η_i and η_j in \mathbb{R}^2 identifies a $d_{i,j} \in [0, d_{max}]$, where d_{max} is the maximal allowable distance in \mathbb{R}^2 , which forms an upper bound to the distances for which $p_{i,j}^{F^*} > 0$ holds, as

$$\begin{aligned} d_{i,j}(t_0) &= |\eta_i(t_0) - \eta_j(t_0)| \\ &= \sqrt{(\varepsilon_i(t_0) - \varepsilon_j(t_0))^2 + ((1 - F_i(t_0)) - (1 - F_j(t_0)))^2}, \end{aligned} \tag{14}$$

and

$$d_{i,j}(t_0 + \Delta t) = |\eta_i(t_0 + \Delta t) - \eta_j(t_0 + \Delta t)| \leq d_{max}, \tag{15}$$

where

$$\eta_i(t_0 + \Delta t) = \eta_i(t_0) + \Omega_i(t_0, \Delta t), \tag{16}$$

where

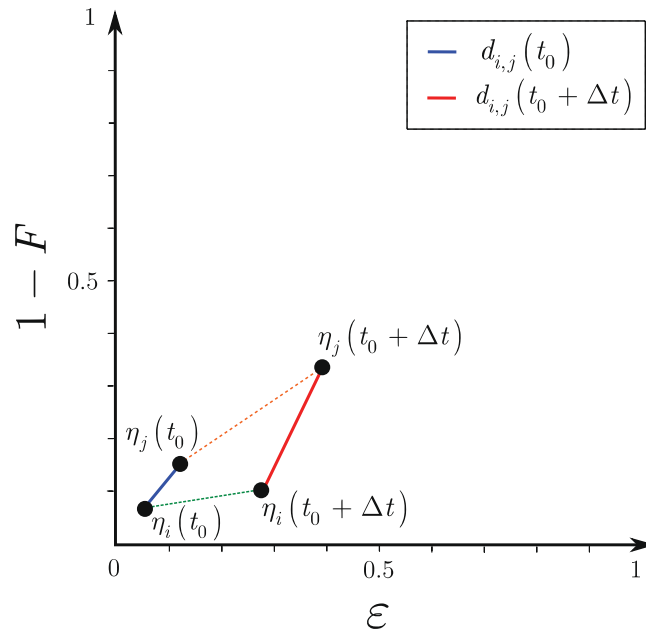


Figure 2. Evolution of the $d_{i,j}(t_0)$ and $d_{i,j}(t_0 + \Delta t)$ distances in \mathbb{R}^2 with respect to a given node pair (i, j) ; ε is the error probability of the local quantum memory and F is the fidelity of the stored entanglement in the local quantum memory. The initial states (storage starting at t_0) of the nodes (i, j) are identified by $\eta_i(t_0)$ and $\eta_j(t_0)$, the current states at time $t_0 + \Delta t$ of the nodes are $\eta_i(t_0 + \Delta t)$ and $\eta_j(t_0 + \Delta t)$. As $d_{i,j}(t_0 + \Delta t) > d_{\max}$, where d_{\max} is a threshold, the yielding probability is $p_{i,j}^{F^*} = 0$.

$$\eta_i(t_0) = \begin{pmatrix} \zeta_i(t_0) \\ 1 - F_i(t_0) \end{pmatrix} \tag{17}$$

and

$$\Omega_i(t_0, \Delta t) = \begin{pmatrix} \varphi_i(t_0, \Delta t) \\ 1 - F_i(t_0, \Delta t) \end{pmatrix}. \tag{18}$$

The fidelities $F_i(t_0)$ and $F_i(t_0, \Delta t)$ refer to the fidelities of stored entanglement in a node i at t_0 and $t_0, \Delta t$, respectively, with relation for nodes (i, j)

$$1 - F_{i,j}(t_0 + \Delta t) = |(1 - F_i(t_0 + \Delta t)) - (1 - F_j(t_0 + \Delta t))| \leq 1 - F_{\Delta}, \tag{19}$$

where $F_{i,j}$ is the difference of entanglement fidelities F_i and F_j , while F_{Δ} is an upper bound on the fidelity difference.

From equation (15), the following relation holds for $p_{i,j}^{F^*}$:

$$p_{i,j}^{F^*} = \begin{cases} p_{i,j}^{F^*} > 0, & \text{if } d_{i,j}(t_0 + \Delta t) \leq d_{\max}, \\ p_{i,j}^{F^*} = 0, & \text{otherwise.} \end{cases} \tag{20}$$

Figure 2 illustrates the evolution of the error probabilities of the local quantum memories and the fidelities of the stored entangled states. Time t_0 refers to the start of storage in the quantum memory and time $t_0 + \Delta t$ is the current time. The distance $d_{i,j}(t_0 + \Delta t)$ measures the difference of $\eta_i(t_0 + \Delta t)$ and $\eta_j(t_0 + \Delta t)$ of a node pair (i, j) . From the time evolution of the error probability of the quantum memory, it follows that $\varepsilon(t_0 + \Delta t) > \varepsilon(t_0)$, and $F(t_0 + \Delta t) < F(t_0)$ holds for the time evolution of the fidelity of the stored entanglement.

The normalized increase of distance $d_{i,j}$ between nodes therefore yields a quantity $\omega_{i,j}, \omega_{i,j} \in [0, 1]$, which characterizes the usability of a stored entanglement in (i, j) from t_0 to $t_0 + \Delta t$, as

$$\omega_{i,j} = 1 - \frac{1}{d_{\max}} \min \left\{ \sqrt{(\varphi_i(t_0, t_0 + \Delta t) - \varphi_j(t_0, t_0 + \Delta t))^2 + (1 - F_i(t_0, t_0 + \Delta t) - (1 - F_j(t_0, t_0 + \Delta t)))^2}, d_{\max} \right\}. \tag{21}$$

As $\omega_{i,j} = 1$, if no change occurs in the initial distance $d_{i,j}(t_0)$ in \mathbb{R}^2 , thus

$$d_{i,j}(t_0 + \Delta t) \approx d_{i,j}(t_0), \tag{22}$$

while $\omega_{i,j} = 0$, if

$$d_{i,j}(t_0 + \Delta t) > d_{\max}, \tag{23}$$

so the yielding relation between $p_{i,j}^{F^*}$ and $\omega_{i,j}$ is

$$p_{i,j}^{F^*} = \begin{cases} p_{i,j}^{F^*} = \max, & \text{if } \omega_{i,j} = 1, \\ 0 < p_{i,j}^{F^*} < \max, & \text{if } \omega_{i,j} < 1, \\ p_{i,j}^{F^*} = 0, & \text{if } \omega_{i,j} = 0. \end{cases} \tag{24}$$

Equation (21) also characterizes the future behavior of the quantum memories in the nodes, i.e., the predictability of the error model of the quantum memories after a given time after beginning storage. The highest values of $\omega_{i,j}$ are therefore assigned to those memory units for which the error probabilities and the entanglement fidelities evolve by a given pattern.

For a given path \mathcal{P} with A_{δ,U_k} and B_{δ,U_k} as the source and target nodes, respectively, associated with a demand δ of user $U_k, k = 1, \dots, K$, where K is the number of users; thus, the overall usability coefficient $\omega_{A_{\delta,U_k},B_{\delta,U_k}}$ for \mathcal{P} is

$$\omega_{A_{\delta,U_k},B_{\delta,U_k}} = \prod_{(i,j) \in \mathcal{P}} \omega_{i,j}. \tag{25}$$

To determine those quantum nodes for which both $\omega_{i,j}$ (21) and $p_{i,j}^{F^*}$ are high, a redefined cost function, $c_{i,j}$, can be defined for a given (i, j) as

$$c_{i,j} = \frac{1}{p_{i,j}^{F^*} \omega_{i,j}}, \tag{26}$$

which assigns the lowest cost to those node pairs for which $\omega_{i,j}$ and $p_{i,j}^{F^*}$ are high.

The remaining quantities from equations (7) and (9) can therefore be rewritten as

$$c_{i,D_i} = \frac{1}{1 - \prod_{j \in D_i} (1 - p_{i,j}^{F^*} \omega_{i,j})}, \tag{27}$$

and

$$\phi'_{i,j} = \frac{p_{i,j}^{F^*} \omega_{i,j} \prod_{k=1}^{j-1} (1 - p_{i,k}^{F^*} \omega_{i,k})}{1 - \prod_{j \in D_i} (1 - p_{i,j}^{F^*} \omega_{i,j})}, \tag{28}$$

which yields the redefined cost of equation (8) as

$$c_{D_p,B} = \sum_{j \in D_i} \phi'_{i,j} f(p_{j,B}^{F^*}). \tag{29}$$

The total cost between i and B such that $F^* \geq F_{crit}$ holds for all entangled contacts between quantum nodes i and B is therefore^{65,66}

$$c_{i,B} = c_{i,D_i} + c_{D_p,B}. \tag{30}$$

Opportunistic Entanglement Distribution. The aim of the opportunistic entanglement distribution algorithm \mathcal{A}_O is to determine a shortest path \mathcal{P}^* with respect to our cost function. The shortest path \mathcal{P}^* contains those node pairs for which $\omega_{i,j}$ and $p_{i,j}^{F^*}$ are maximal, and therefore the resulting cost function (26) is the lowest in a quantum network N . Thus, the algorithm finds the repeater nodes for entanglement distribution by maximizing the usability of stored entanglement.

Some preliminary notations for the algorithm are as follows. Let A_{δ,U_k} and B_{δ,U_k} be the source and target nodes, respectively, associated with a demand δ of user U_k . The algorithm selects those nodes that provide the lowest cost with respect to $c_{i,j}$ for a given (i, j) to distribute entanglement from A_{δ,U_k} to B_{δ,U_k} . Assume that for a set S' of nodes there exists a path to B_{δ,U_k} in a quantum network $N = (V, S)$. Let \tilde{S} refer to a set of nodes for which the shortest path to B_{δ,U_k} is not yet determined.

The \mathcal{A}_O algorithm of the minimal-cost opportunistic entanglement distribution is detailed in Algorithm 1.

Computational Complexity. The computational complexity of the minimal-cost \mathcal{A}_O opportunistic entanglement distribution is as follows.

Let $N = (V, E)$ be a quantum repeater network with $|V|$ quantum nodes. Applying a \mathcal{L} logarithmic search⁶⁷ to find a node with an actual minimal cost requires at most

$$\mathcal{O}(\log |V|) \tag{31}$$

steps, via $\mathcal{O}(\log |V|)$ comparisons.

Algorithm 1. \mathcal{A}_O : Minimal-cost opportunistic entanglement distribution.

- Step 1.** For all quantum node $i \in V$, initial cost $f(p_{i,B_{\delta,U_k}}^{F^*}) = \infty$ and $\mathcal{D}_i = 0$, where $f(p_{i,B_{\delta,U_k}}^{F^*})$ is the cost of a path from i to B_{δ,U_k} , while $\mathcal{D}_i = 0$ is the distributing set associated to node i to reach B_{δ,U_k} . Set $\tilde{S} = V$ with cost $f(p_{i \in \tilde{S}, B_{\delta,U_k}}^{F^*}) = 0$, and set $S' = \emptyset$.
- Step 2.** Determine the final cost of the path with respect to a node Φ_n from set \tilde{S} with minimal cost $\tilde{f}(p_{\Phi_n, B_{\delta,U_k}}^{F^*})$, where $\tilde{f}(\cdot)$ is an upper bound on the cost of the shortest path from Φ_n to B_{δ,U_k} , while node Φ_n is determined as $\Phi_n = \min_{z \in \tilde{S}} f(p_{z, B_{\delta,U_k}}^{F^*})$, where z is a node from set S' .
- Step 3.** Set $S' = S' \cup \{\Phi_n\}$, and for each (i, Φ_n) set $\mathcal{D} = \mathcal{D}_i \cup \{\Phi_n\}$, where \mathcal{D} is a distributing set.
- Step 4.** If $f(p_{i, B_{\delta,U_k}}^{F^*}) > \tilde{f}(p_{\Phi_n, B_{\delta,U_k}}^{F^*})$, update the cost of node i as $f(p_{i, B_{\delta,U_k}}^{F^*}) = c_{i, \mathcal{D}_i} + c_{\mathcal{D}_i, B_{\delta,U_k}}$, and set $\mathcal{D}_i = \mathcal{D}$.
- Step 5.** Repeat steps 2-4, until $\tilde{S} \neq \emptyset$.
- Step 6.** Output the minimal cost path \mathcal{P}^* between i_{δ,U_k} and B_{δ,U_k} .

Since the number of nodes is $|V|$, setting the final path cost for all quantum nodes requires at most

$$\mathcal{O}(|V|) \quad (32)$$

steps.

From (31) and (32) follows straightforwardly that the complexity of the minimal-cost opportunistic entanglement distribution algorithm is bounded above by

$$\mathcal{O}(|V| \log |V|). \quad (33)$$

Conclusions

Here we defined a method for entanglement distribution in the quantum Internet. Our method utilizes distributing sets for quantum nodes, which can preserve quantum entanglement with the highest fidelity in their local quantum memories. The algorithm is opportunistic, since in each iteration step a node is selected from a distributing set that can provide optimal conditions. The cost function includes the utilization of the evolution of the error model of the local quantum memories, and the fidelities of the stored entangled states. A usability parameter quantifies the predictability of the evolution of the error model, and of the evolution of the entanglement fidelity. The computational complexity of the method is moderate, which allows for direct application in experimental quantum Internet scenarios and in long-distance quantum communications.

Data Availability

This work does not have any experimental data.

References

1. Van Meter, R. *Quantum Networking*. ISBN 1118648927, 9781118648926 (John Wiley and Sons Ltd, 2014).
2. Van Meter, R., Ladd, T. D., Munro, W. J. & Nemoto, K. System Design for a Long-Line Quantum Repeater. *IEEE/ACM Transactions on Networking* **17**(3), 1002–1013 (2009).
3. Van Meter, R., Satoh, T., Ladd, T. D., Munro, W. J. & Nemoto, K. Path selection for quantum repeater networks. *Networking Science* **3**(1–4), 82–95 (2013).
4. Gyongyosi, L., Imre, S. & Nguyen, H. V. A Survey on Quantum Channel Capacities. *IEEE Communications Surveys and Tutorials*, <https://doi.org/10.1109/COMST.2017.2786748> (2018).
5. Lloyd, S. *et al.* Infrastructure for the quantum Internet. *ACM SIGCOMM Computer Communication Review* **34**, 9–20 (2004).
6. Kimble, H. J. The quantum Internet. *Nature* **453**, 1023–1030 (2008).
7. Van Meter, R. & Devitt, S. J. Local and Distributed Quantum Computation. *IEEE Computer* **49**(9), 31–42 (2016).
8. Gyongyosi, L. & Imre, S. Decentralized Base-Graph Routing for the Quantum Internet, *Physical Review A*, <https://doi.org/10.1103/PhysRevA.98.022310> (American Physical Society, 2018).
9. Gyongyosi, L. & Imre, S. Dynamic topology resilience for quantum networks. *Proc. SPIE 10547*, Advances in Photonics of Quantum Computing, Memory, and Communication XI, 105470Z, <https://doi.org/10.1117/12.2288707> (22 February 2018).
10. Gyongyosi, L. & Imre, S. Topology Adaption for the Quantum Internet. *Quantum Information Processing*, <https://doi.org/10.1007/s11128-018-2064-x> (Springer Nature, 2018).
11. Pirandola, S., Laurenza, R., Ottaviani, C. & Banchi, L. Fundamental limits of repeaterless quantum communications, *Nature Communications*, 15043, <https://doi.org/10.1038/ncomms15043> (2017).
12. Pirandola, S. *et al.* Theory of channel simulation and bounds for private communication. *Quantum Sci. Technol.* **3**, 035009 (2018).
13. Pirandola, S. Capacities of repeater-assisted quantum communications. *arXiv:1601.00966* (2016).
14. Laurenza, R. & Pirandola, S. General bounds for sender-receiver capacities in multipoint quantum communications. *Phys. Rev. A* **96**, 032318 (2017).
15. Gyongyosi, L. & Imre, S. A Survey on Quantum Computing Technology. *Computer Science Review*, <https://doi.org/10.1016/j.cosrev.2018.11.002>, ISSN: 1574-0137 (Elsevier, 2018).
16. Gyongyosi, L. & Imre, S. Multilayer Optimization for the Quantum Internet. *Scientific Reports*, <https://doi.org/10.1038/s41598-018-30957-x> (Nature, 2018).
17. Gyongyosi, L. & Imre, S. Entanglement Availability Differentiation Service for the Quantum Internet. *Scientific Reports*, <https://doi.org/10.1038/s41598-018-28801-3>, <https://www.nature.com/articles/s41598-018-28801-3> (Nature, 2018).
18. Gyongyosi, L. & Imre, S. Entanglement-Gradient Routing for Quantum Networks. *Scientific Reports*, <https://doi.org/10.1038/s41598-017-14394-w>, <https://www.nature.com/articles/s41598-017-14394-w> (Nature, 2017).
19. Imre, S. & Gyongyosi, L. *Advanced Quantum Communications - An Engineering Approach*. (New Jersey, Wiley-IEEE Press, 2013).
20. Caleffi, M. End-to-End Entanglement Rate: Toward a Quantum Route Metric, 2017 *IEEE Globecom*, <https://doi.org/10.1109/GLOCOMW.2017.8269080> (2018).
21. Caleffi, M. Optimal Routing for Quantum Networks. *IEEE Access* Vol 5, <https://doi.org/10.1109/ACCESS.2017.2763325> (2017).

22. Caleffi, M., Cacciapuoti, A. S. & Bianchi, G. Quantum Internet: from Communication to Distributed Computing. *arXiv:1805.04360* (2018).
23. Castelvocchi, D. The quantum internet has arrived. *Nature*, <https://www.nature.com/articles/d41586-018-01835-3> (News and Comment, 2018).
24. Cacciapuoti, A. S. *et al.* Quantum Internet: Networking Challenges in Distributed Quantum Computing. *arXiv:1810.08421* (2018).
25. Kok, P. *et al.* Linear optical quantum computing with photonic qubits. *Rev. Mod. Phys.* **79**, 135–174 (2007).
26. Petz, D. *Quantum Information Theory and Quantum Statistics* (Springer-Verlag, Heidelberg, Hiv: 6, 2008).
27. Bacsardi, L. On the Way to Quantum-Based Satellite Communication. *IEEE Comm. Mag.* **51**(08), 50–55 (2013).
28. Muralidharan, S., Kim, J., Lutkenhaus, N., Lukin, M. D. & Jiang, L. Ultrafast and Fault-Tolerant Quantum Communication across Long Distances. *Phys. Rev. Lett.* **112**, 250501 (2014).
29. Biamonte, J. *et al.* Quantum Machine Learning. *Nature* **549**, 195–202 (2017).
30. Lloyd, S., Mohseni, M. & Rebentrost, P. Quantum algorithms for supervised and unsupervised machine learning. *arXiv:1307.0411* (2013).
31. Lloyd, S., Mohseni, M. & Rebentrost, P. Quantum principal component analysis. *Nature Physics* **10**, 631 (2014).
32. Lloyd, S. Capacity of the noisy quantum channel. *Physical Rev. A* **55**, 1613–1622 (1997).
33. Lloyd, S. The Universe as Quantum Computer. *A Computable Universe: Understanding and exploring Nature as computation*, Zenil, H. ed., *arXiv:1312.4455v1* (World Scientific, Singapore, 2013).
34. Shor, P. W. Scheme for reducing decoherence in quantum computer memory. *Phys. Rev. A* **52**, R2493–R2496 (1995).
35. Chou, C. *et al.* Functional quantum nodes for entanglement distribution over scalable quantum networks. *Science* **316**(5829), 1316–1320 (2007).
36. Yuan, Z. *et al.* Experimental demonstration of a BDCZ quantum repeater node *Nature* **454**, 1098–1101 (2008).
37. Kobayashi, H., Le Gall, F., Nishimura, H. & Rotteler, M. General scheme for perfect quantum network coding with free classical communication. *Lecture Notes in Computer Science* (Automata, Languages and Programming SE-52 vol. 5555) pp 622–633 (Springer, 2009).
38. Hayashi, M. Prior entanglement between senders enables perfect quantum network coding with modification, *Physical Review A* Vol. 76, 040301(R) (2007).
39. Hayashi, M., Iwama, K., Nishimura, H., Raymond, R. & Yamashita, S. Quantum network coding. *Lecture Notes in Computer Science* (STACS 2007 SE52 vol. 4393) eds Thomas, W. & Weil, P. (Berlin Heidelberg: Springer, 2007).
40. Chen, L. & Hayashi, M. Multicopy and stochastic transformation of multipartite pure states. *Physical Review A* **83**(No. 2), 022331 (2011).
41. Schoute, E., Mancinska, L., Islam, T., Kerenidis, I. & Wehner, S. Shortcuts to quantum network routing. *arXiv:1610.05238* (2016).
42. Lloyd, S. & Weedbrook, C. Quantum generative adversarial learning. *Phys. Rev. Lett.* **121**, arXiv:1804.09139 (2018).
43. Gisin, N. & Thew, R. Quantum Communication. *Nature Photon.* **1**, 165–171 (2007).
44. Xiao, Y. F. & Gong, Q. Optical microcavity: from fundamental physics to functional photonics devices. *Science Bulletin* **61**, 185–186 (2016).
45. Briegel, H. J., Dur, W., Cirac, J. I. & Zoller, P. Quantum repeaters: the role of imperfect local operations in quantum communication. *Phys. Rev. Lett.* **81**, 5932–5935 (1998).
46. Dur, W., Briegel, H. J., Cirac, J. I. & Zoller, P. Quantum repeaters based on entanglement purification. *Phys. Rev. A* **59**, 169–181 (1999).
47. Duan, L. M., Lukin, M. D., Cirac, J. I. & Zoller, P. Long-distance quantum communication with atomic ensembles and linear optics. *Nature* **414**, 413–418 (2001).
48. Van Loock, P. *et al.* Hybrid quantum repeater using bright coherent light. *Phys. Rev. Lett.* **96**, 240501 (2006).
49. Zhao, B., Chen, Z. B., Chen, Y. A., Schmiedmayer, J. & Pan, J. W. Robust creation of entanglement between remote memory qubits. *Phys. Rev. Lett.* **98**, 240502 (2007).
50. Goebel, A. M. *et al.* Multistage Entanglement Swapping. *Phys. Rev. Lett.* **101**, 080403 (2008).
51. Simon, C. *et al.* Quantum Repeaters with Photon Pair Sources and Multimode Memories. *Phys. Rev. Lett.* **98**, 190503 (2007).
52. Tittel, W. *et al.* Photon-echo quantum memory in solid state systems. *Laser Photon. Rev.* **4**, 244–267 (2009).
53. Sangouard, N., Dubessy, R. & Simon, C. Quantum repeaters based on single trapped ions. *Phys. Rev. A* **79**, 042340 (2009).
54. Dur, W. & Briegel, H. J. Entanglement purification and quantum error correction. *Rep. Prog. Phys.* **70**, 1381–1424 (2007).
55. Sheng, Y. B. & Zhou, L. Distributed secure quantum machine learning. *Science Bulletin* **62**, 1025–1019 (2017).
56. Leung, D., Oppenheim, J. & Winter, A. Quantum network communication; the butterfly and beyond. *IEEE Trans. Inf. Theory* **56**, 3478–90 (2010).
57. Kobayashi, H., Le Gall, F., Nishimura, H. & Rotteler, M. Perfect quantum network communication protocol based on classical network coding. *Proceedings of 2010 IEEE International Symposium on Information Theory (ISIT)* pp 2686–90 (2010).
58. Zhang, W. *et al.* Quantum Secure Direct Communication with Quantum Memory. *Phys. Rev. Lett.* **118**, 220501 (2017).
59. Enk, S. J., Cirac, J. I. & Zoller, P. Photonic channels for quantum communication. *Science* **279**, 205–208 (1998).
60. Shor, P. W. Fault-tolerant quantum computation. *37th Symposium on Foundations of Computing* pp. 56–65 (IEEE Computer Society Press, 1996).
61. Jozsa, R. Fidelity for Mixed Quantum States. *J. Mod. Optics* **41**, 2315 (1995).
62. Nielsen, M. A. The entanglement fidelity and quantum error correction. *arXiv:quant-ph/9606012* (1996).
63. Schumacher, B. Sending quantum entanglement through noisy channels. *Phys Rev A* **54**(4), 2614–2628 (1996).
64. Fedrizzi, A. *et al.* High-fidelity transmission of entanglement over a high-loss free-space channel. *Nature Physics* **5**(6), 389–392 (2009).
65. Leepila, R. *Routing Schemes for Survivable and Energy-Efficient Networks*, PhD Thesis (Department of Information and Communication Engineering, The University of Electro-Communications, 2014).
66. Rak, J. *Resilient Routing in Communication Networks* (Springer, 2015).
67. Knuth, D. Sorting and searching. *The Art of Computer Programming*, ISBN 978-0-201-89685-5 (Addison-Wesley Professional, 1998).

Acknowledgements

This work was partially supported by the European Research Council through the Advanced Fellow Grant, in part by the Royal Society’s Wolfson Research Merit Award, in part by the Engineering and Physical Sciences Research Council under Grant EP/L018659/1, by the Hungarian Scientific Research Fund - OTKA K-112125, and by the National Research Development and Innovation Office of Hungary (Project No. 2017-1.2.1-NKP-2017-00001), and in part by the BME Artificial Intelligence FIKP grant of EMMI (BME FIKP-MI/SC).

Author Contributions

L.G.Y. designed the protocol and wrote the manuscript. L.G.Y. and S.I. analyzed the results. All authors reviewed the manuscript.

Additional Information

Competing Interests: The authors declare no competing interests.

Publisher's note: Springer Nature remains neutral with regard to jurisdictional claims in published maps and institutional affiliations.



Open Access This article is licensed under a Creative Commons Attribution 4.0 International License, which permits use, sharing, adaptation, distribution and reproduction in any medium or format, as long as you give appropriate credit to the original author(s) and the source, provide a link to the Creative Commons license, and indicate if changes were made. The images or other third party material in this article are included in the article's Creative Commons license, unless indicated otherwise in a credit line to the material. If material is not included in the article's Creative Commons license and your intended use is not permitted by statutory regulation or exceeds the permitted use, you will need to obtain permission directly from the copyright holder. To view a copy of this license, visit <http://creativecommons.org/licenses/by/4.0/>.

© The Author(s) 2019